

Flavin Monooxygenase Metabolism: Why Medicinal Chemists Should Matter

Gabriele Cruciani,^{*,†} Aurora Valeri,[‡] Laura Goracci,[†] Roberto Maria Pellegrino,[‡] Federica Buonerba,[‡] and Massimo Baroni[§]

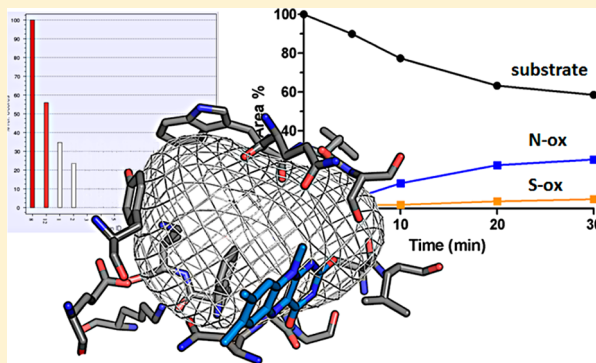
[†]Laboratory for Chemoinformatics and Molecular Modelling, Department of Chemistry, Biology and Biotechnology, University of Perugia, Via Elce di Sotto 8, 06123 Perugia, Italy

[‡]Department of Chemistry, Biology and Biotechnology, University of Perugia, Via Elce di Sotto 8, 06123 Perugia, Italy

[§]Molecular Discovery, 215 Marsh Road, Pinner, HA55NE, London, U.K.

S Supporting Information

ABSTRACT: FMO enzymes (FMOs) play a key role in the processes of detoxification and/or bioactivation of specific pharmaceuticals and xenobiotics bearing nucleophilic centers. The *N*-oxide and *S*-oxide metabolites produced by FMOs are often active metabolites. The FMOs are more active than cytochromes in the brain and work in tandem with CYP3A4 in the liver. FMOs might reduce the risk of phospholipidosis of CAD-like drugs, although some FMOs metabolites seem to be neurotoxic and hepatotoxic. However, *in silico* methods for FMO metabolism prediction are not yet available. This paper reports, for the first time, a substrate-specificity and catalytic-activity model for FMO3, the most relevant isoform of the FMOs in humans. The application of this model to a series of compounds with unknown FMO metabolism is also reported. The model has also been very useful to design compounds with optimal clearance and in finding erroneous literature data, particularly cases in which substances have been reported to be FMO3 substrates when, in reality, the experimentally validated *in silico* model correctly predicts that they are not.



INTRODUCTION

Flavin containing monooxygenases (FMOs) are an important component in the arsenal of enzymes that metabolize drugs, as they complement the work performed on xenobiotics by the P450 enzymes. While the P450 enzymes tend to primarily oxidize molecules through electrophilic reactions, principally through radical intermediates, the FMO enzymes tend to oxidize the same molecules through nucleophilic addition reactions.^{1,2} Discovered in the 1960s,³ this system of hepatic microsomal enzymes uses NADPH and oxygen to convert molecules containing primarily nucleophilic centers, in particular nitrogen, sulfur, phosphorus, and selenium atoms, all of which have a free lone pair of electrons, into the corresponding oxides. Besides oxidizing the same atoms, the cytochromes P450 directly oxidize carbon atoms readily. This implies that the FMO enzymes metabolize a more restricted range of compounds than the cytochromes P450. Recently, Testa et al.⁴ have shown that the FMOs are responsible for about 2.5% of all metabolic reactions and therefore about 6% of all the phase I metabolic reactions. Since FMO3 is the isoform of FMO that is most dominant in the liver of human adults, almost all the reactions of pharmaceutical interest are mediated by this enzyme. FMO3 is the major representative of the FMO

family, just as CYP3A4 is the major representative of the cytochrome family.

The experimental work being presented here aimed at proving that the importance of the FMOs, and in particular that of FMO3, remains underestimated. Many oxidation reactions that in the past have been attributed to CYP3A4 are in reality performed solely by, or in part by, FMO3. We believe that the FMOs are more frequently responsible for a number of these reactions than is currently attributed to them and that the role played by the principal isoform FMO3 is second only to the few cytochrome P450s considered to be the most important. As an example, the metabolism of a few selected compounds will be discussed. Arbidol, an antiviral agent, is a CYP3A4 substrate. It has been shown recently that this drug first reacts with FMO3 (*S*-oxidation) to give the sulfoxide metabolite and that the resulting metabolite undergoes subsequent *N*-demethylation by CYP3A4.⁵ Benzydamine is an anti-inflammatory agent whose elimination pathway in the human body can be primarily attributed to FMO3.⁶ Moclobemide is a reversible MAO inhibitor of which the *N*-oxide, formed through FMO3 catalysis, is the primary metabolite.⁷ Itopride, a gastroprokinetic

Received: May 7, 2014

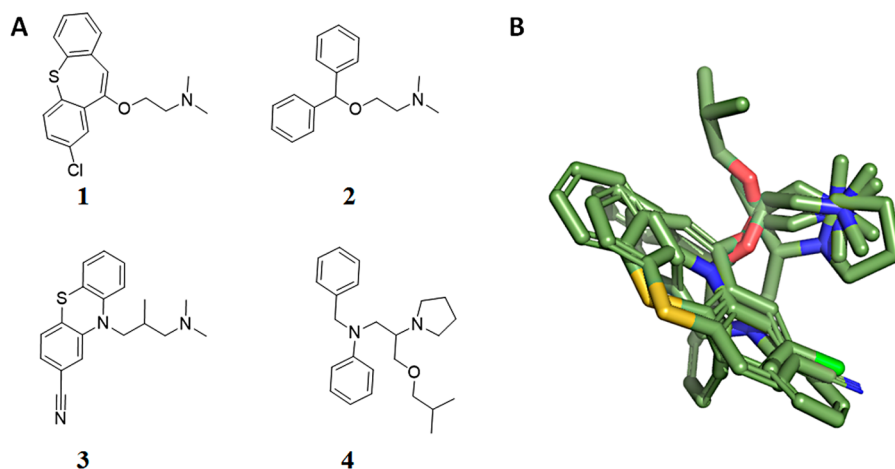


Figure 1. (A) Structures of zotepine (1), diphenidramine (2), cyamemazine (3), and bepridil (4). Compound 1 is a known FMO3 substrate.²³ Compound 2, incubated in recombinant FMO3, is an FMO3 substrate, while 3 and 4 proved to be nonsubstrates. (B) Superimposition of the chemical structures of 1–4. Their 3D structures are very similar, with a good alignment of the tertiary amine nitrogen atoms and of the aromatic moieties.

agent, has a metabolic clearance that is practically all caused by FMO3.⁸ The *N*-oxide ranitidine metabolite, which blocks histamine H₂ receptors, is formed exclusively by FMO3.⁹ Other examples in which the catalysis of FMO enzymes (including FMO3) is important, though not necessarily dominant in the overall clearance, are olanzapine,¹⁰ pargyline,¹¹ xanomeline,¹² zimelidine,¹³ and many others. However, limited information about other drugs is provided in the literature. Imipramine has not been considered to be a substrate of FMO3,¹⁴ even though other sources classify it as an optimal substrate.¹⁵ Preliminary studies indicated that diphenhydramine, a known substrate of CYP2D6,¹⁶ is actually a better substrate of FMO3 for *N*-oxidation, while CYP2D6 (and in a minor extent CYP3A4) mainly generates the *N*-dealkylated metabolite (see Figure S1, Supporting Information). In the past, diphenhydramine was only reported to be a substrate for porcine FMO1 to give the *N*-oxide metabolite.^{17,18} In addition to diphenhydramine, ziprasidone, besides being metabolized by CYP3A4, also proved to be an optimal substrate for FMO3 (Table S1, Supporting Information). It must be noticed that among the drugs reported above, ranitidine, zimelidine, olanzapine, imipramine, and ziprasidone are phospholipidosis (PLD) inducers,¹⁹ although for ziprasidone and olanzapine medium confidence data are available.²⁰ Recently the importance of metabolism in PLD induction has been reported,^{19,21,22} although metabolism by FMO3 has not been related to phospholipidosis effect so far.

As the next paragraphs will demonstrate, it is not simple to understand whether a xenobiotic is a substrate of the FMOs or not, especially for FMO3. It is also difficult to predict the site of oxidation and any potential competition with CYP3A4. *In silico* methods can be extremely useful in helping the researcher formulate hypothesis and explain/interpret experiments of metabolite identification.

While *in silico* models that reproduce in part the behavior of human cytochromes are currently available, nothing has been developed so far for substrate specificity prediction and site of oxidation prediction for xenobiotics that interact with FMO. This work reports, for the first time, a simulation model that is capable of predicting the substrate specificity and the site of metabolism for the isoform that is most relevant to medicinal chemistry: the FMO3 isoform. Some examples of the

applications of this simulation model and tests of its predictive ability in compounds of which the FMO metabolism has never been reported are also presented.

RESULTS AND DISCUSSION

FMO3 Substrate Selectivity and SoM. To a casual observer the task of deciding which metabolic reactions the FMO enzymes can perform on a substrate might seem trivial. The real situation is obviously much more complex than simple appearances. Zotepine (1) (see Figure 1) is known to be an FMO3 substrate.²³ Molecules 2–4 in Figure 1A are structurally similar to zotepine, as shown from alignment in Figure 1B. However, metabolism studies performed using recombinant human FMO3 (see Experimental Section for details, and see Supporting Information for LC/MS data) showed that diphenhydramine (2), like zotepine (1), proved to be an optimal FMO3 substrate, reacting to form the *N*-oxide, while the *N*-dealkylated metabolite was formed upon incubation with recombinant CYP2D6 isoform (Figure S1, Supporting Information). On the other hand, cyamemazine (3) and bepridil (4) did not produce any metabolite at the experimental conditions used, with cyamemazine being a weak substrate only when tested at higher concentration. Since the same reactive group is present in all the molecules, the reason for the observed difference should not be found in the reactivity of these compounds but rather in their diverse exposition of the same functional group or complete lack of interaction with the enzyme. The fact that these molecules are very similar to each other even from a three-dimensional point of view demonstrates that the FMO3–substrate interaction is very specific and very sensitive to small changes in the three-dimensional structure of the substrate.

The same situation arises in small molecules, such as arecoline (5) and alvamine (6), with the latter developed as a bioisoster of the former muscarinic cholinergic compound (Figure 2). Arecoline is an optimal substrate of FMO3,²⁴ while the alvamine is not.²⁵

Another case is presented by phenethylamine (7), which is a good FMO3 substrate,²⁶ while the very similar tetrahydroisoquinoline (8) was only a very weak substrate (Figure 3), according to the experimental findings (LC/MS metabolism data for all compounds proved to be substrates for FMO3 in

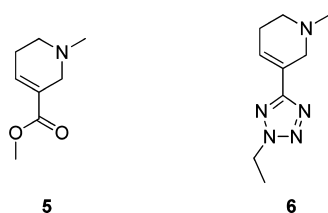


Figure 2. Arecoline (5) and its bioisoster alvamine (6). The former is an optimal substrate of FMO3, while the latter is not.

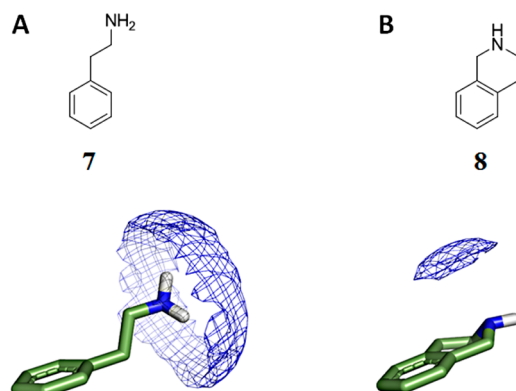


Figure 3. Phenethylamine (A), a FMO3 substrate, compared with tetrahydroisoquinoline (B), which is not a FMO3 substrate. The GRID MIF shows favorable energetic interactions with hydroperoxyflavin group.

this section are reported in Table S1, Supporting Information). The GRID force field²⁷ shows that the hydroperoxyflavin group in phenethylamine can produce a favorable electrophilic reaction in a much larger volume than tetrahydroisoquinoline, and therefore the geometric control is less tight.

These last two cases show that FMO3, unlike CYP3A4 that performs the same reactions, is selective even with small molecules. It is evident that the productive spatial interaction with the enzyme (favorable enzyme recognition) plays a key role and is probably more important than chemical reactivity. From all these examples it emerges that it is not at all simple to predict whether a compound is a substrate of FMO3 or not. Obviously, if this information was available in literature, predicting the site of metabolism (SoM) might seem a simple task. Since the FMO reactions are more limited than those of P450, it is definitely easier to predict the SoM for the FMOs than for the P450s. Even so, a superficial treatment will not suffice, since the correct prediction might be more difficult than previously thought. On the basis of these considerations, a number of compounds possessing two or three potential sites of oxidation were selected for testing. Compound 9 in Figure 4 has three potential centers for N-oxidation. The most nucleophilic center, which is also the most potentially reactive one, is represented by the imine nitrogen. However, we found

that the reaction happens exclusively in the nitrogen atom of the terminal tertiary amine, even though this center is less nucleophilic, as demonstrated by the presence of the fragment with m/z 187.12 in the MSMS spectrum of the metabolite. Compound 10 has two potential centers for N-oxidation. The most nucleophilic center is the quinuclidine group, which is exactly where the only N-oxidation reaction happens, as the fragment with m/z 154.0 proves. Cimetidine (11) has two centers of similar nucleophilicity. The oxidation reaction happens at the sulfur atom, according to the MSMS fragments with m/z 95.06 and 99.06, among the others. As with the cytochrome P450s, even in this case the oxidation reaction happens as a combination of substrate reactivity (caused in this case by its nucleophilicity) and by the productive spatial interaction with the enzyme (favorable enzyme recognition). Evaluating these two factors separately is not simple. Furthermore, it is even more complicated to evaluate the importance that the enzyme attributes to either component.

The importance of pure chemical reactivity can be described using two very similar compounds which will probably be exposed in the FMO3 catalytic site in a very similar manner. Compounds 12 and 13 in Figure 5 were acquired and tested,

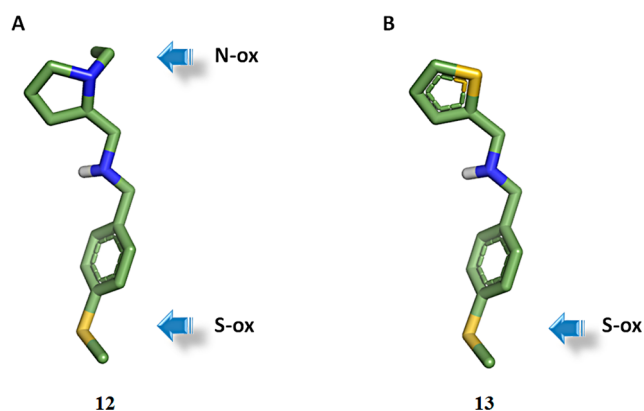


Figure 5. Compounds 12 (A) and 13 (B) are similar FMO3 substrates that react in a different manner. The former reacts at the sulfur atom of the methylsulfide and at the pyrrolidine nitrogen, while the latter reacts only at the methylsulfide moiety.

both being FMO3 substrates. The former reacts at the sulfur atom of the methylsulfide and at the pyrrolidine nitrogen, while the latter reacts only at the methylsulfide moiety. This difference can be explained by the different nucleophilicity of the pyrrolidine and thiophene moieties. As reported later in Computational Section, the pyrrolidine moiety is a strong nucleophilic group, while the thiophene moiety is only very weakly nucleophilic. We may therefore conclude that compounds will be hardly metabolized by FMO3 enzyme in thiophene groups, especially when better nucleophilic moieties are present in the molecules.

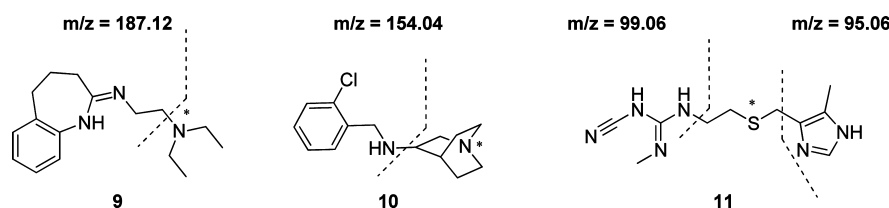


Figure 4. Experimental sites of metabolism (oxidation) for compounds 9–11 are marked with asterisks.

Furthermore, as reported above, cases in which FMO3 generates more than one reaction are not rare. In such cases, the prediction of the fastest, or most important reaction, is made even more difficult. Would the reader be able to predict the site of oxidation responsible for the fastest generation of the metabolite by FMO3 for the molecules in Figure 6?

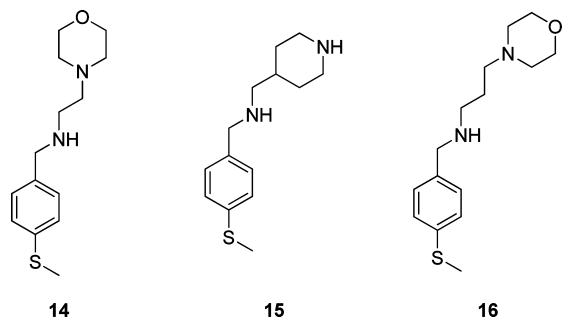


Figure 6. Predicting the correct rank for sites of metabolism (SoM) in compounds 14–16 by FMO3 is not a simple task.

FMO3: 3D Structure. FMO3 is the dominant form of FMO in the liver of adult humans. It possesses ample substrate specificity, and it is also the most selective FMO enzyme.

Unfortunately, no structural information at the atomic resolution is available for any microsomal form of FMO enzymes. Nevertheless, high resolution crystalline structures have been published for yeast and for some bacterial isoforms of this enzyme, as shown in the Protein Data Bank (PDB). These isoforms are normally found to be soluble in the cytosol, utilize NADP(H) as a cofactor, and contain conserved sequences for cofactor–protein binding. These soluble enzymes provide a reasonable base from which homology models for the human microsomal FMO enzymes can be produced.

The model presented in the Computational Section of this work suggests that FMOs possess two distinctive domains with FAD and NADP(H) bound close to the interface. From their position in the structure, the nicotinamide ring and the ring adjacent to the ribose in NADP(+) are an integral part of the catalytic site, being actively employed in the stabilization of the oxygenated intermediate. This characteristic suggests that NADP(H) has a fundamental role because of the two binding modes, which allow it to function in the modulation of both reduction and oxidation.

The catalytic cycle demonstrates that the flavone–hydroperoxide (FAD-OOH) species transfers an oxygen atom to the substrate in the first step of the process. The reaction

Table 1. Chemical Structures of FMO3 Substrates⁴²

A			
B			
C			
D			

⁴²It can be noted that the substrates are very diverse, and they show different charge (positive (A), negative (B), zwitterionic (C), neutral (D)), size, shape, hydrophobicity, and polarity. The structures correspond to the predominant species at pH 8.0 (FMO3 works in basic conditions). The computation of the predominant species was carried out using MoKa.^{39,40}

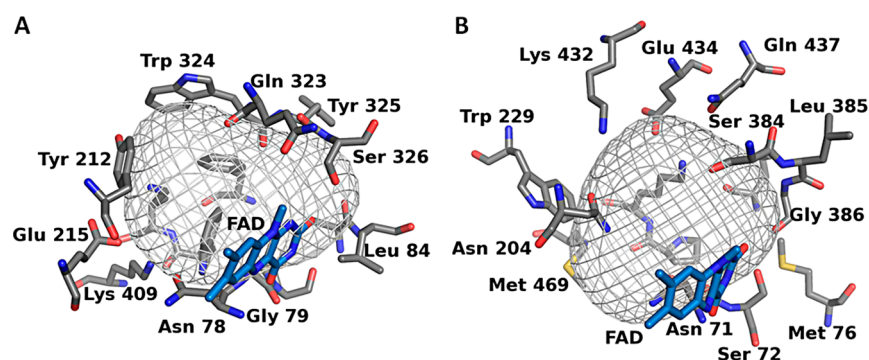


Figure 7. Bacterial (2vq7 structure, A) and human (calculated structure, B) catalytic sites of FMO3. Amino acids that play an important role in substrate orientation are reported. Cavities are computed by FLAP software.^{43,44}

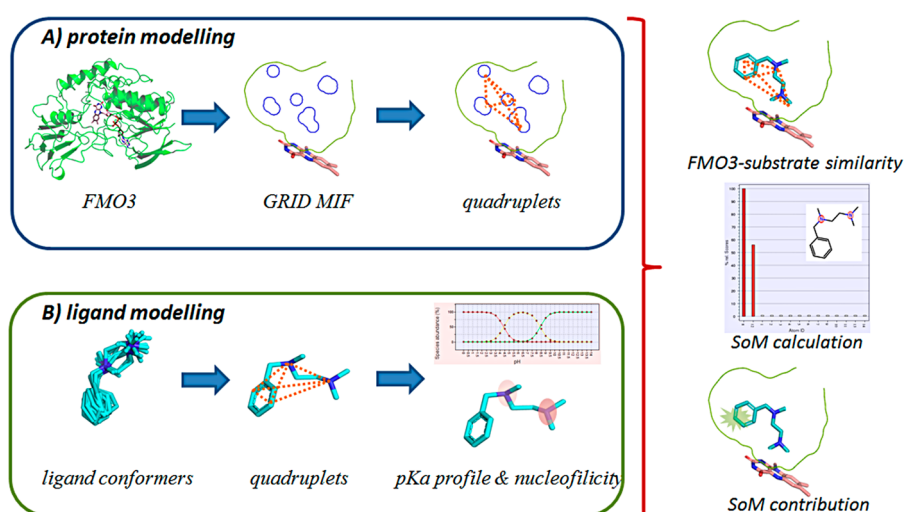


Figure 8. Metasite flowchart for FMO3 SoM calculation.

mechanism is concerted; that is, NADP(H), oxygen, and the oxidable substrate are added to the enzyme before any of the products are released. The release of water and/or NADP(+) is considered to be the limiting step. The flavone–hydroperoxide (FAD-OOH) is a relatively stable species, though with a low oxidative potential. For the oxidation of the FMO substrates to happen, the substrates themselves must be sufficiently nucleophilic and must be able to interact with the enzyme with the right geometry. As with the cytochromes,²⁸ even in this case the oxidation reaction happens by a combination of substrate reactivity (described in this case by its nucleophilicity) and by the productive spatial interaction with the enzyme (favorable enzyme recognition).

Unlike the cytochromes, which exhibit a notable preference in the selection of their substrates (positively charged in the case of CYP2D6, negatively charged in the case of CYP2C9, neutral in the case of CYP3A4), the FMOs do not demonstrate a charge preference in their substrates, as shown in Table 1, which lists some noteworthy substrates of FMO3. It can be noted that neutral, positively charged, and negatively charged substrates are reported.

Even though little is known on how the enzyme controls the access of the substrate to the active site, some hints have emerged from the X-ray structure of the bacterial and yeast forms concerning possible mechanisms for stabilization of the hydroperoxide group in the active site. The FAD group interacts with an asparagine residue (Asn78 in 2vq7, conserved

in all FMOs). It has been suggested that Asn78 stabilizes C4 α -hydroperoxide through polar interactions.⁴¹ It is interesting to note that a polymorphic mutation to this residue in the human form of FMO3 (N to S/K) causes complete loss of function.⁴² Another contribution to the stability of the hydroperoxide could be the NADP(+) bound in the active site. It has been hypothesized that this group shields the hydroperoxide group from interacting with the solvent.⁴¹ Molecular dynamics simulations on a prokaryotic FMO protein (PDB code 2vq7; see computational details) show that the active complex protein–NAD–FAD is stable enough and that the active site of the enzyme is not very flexible. The volume of the active site varies from a minimum of 1000 Å³ to a maximum of 1200 Å³, with an entrance of relatively modest size. Similar findings were obtained when a model for the human protein was used (see computational details in the Experimental Section). This implies that only small to medium-sized substrates may enter. The catalytic site of the enzyme and the amino acids that play an important role in substrate recognition are shown in Figure 7.

Calculation of the FMO3–Substrate Interaction. The function describing the recognition between the FMO3 enzyme and the substrate is based on the FLAP algorithm,⁴³ which has been designed to anchor a flexible substrate in a flexible protein in an extremely rapid manner. The function does not calculate the thermodynamics of the process but rather considers the three-dimensional compatibility between the molecular inter-

Table 2. Nucleophile-Reactivity Parameter in Water Solvent^a

compd	exptl ^b	calcd	compd	exptl ^b	calcd
1,2-ethanediamine	13.3	13.5	glycineamide	12.3	12.0
1,3-diaminopropane	14.0	14.4	glycinenitrile	10.8	10.4
1-methyluracil (anion)	8.5	9.8	hydroxylamine	11.4	11.6
2-formylimidazole (anion)	11.1	13.1	isopropylamine	12.0	13.6
2-pyridone (anion)	12.5	11.9	methyl-2-aminoacetate	12.1	10.8
4-methylpyridine	11.1	11.4	methylamine	13.8	13.1
4-(dimethylamino)pyridine	13.2	14.3	methylhydrazine	17.2	16.0
4-aminopyridine	12.2	12.2	morpholine	15.6	15.6
4-chloropyridine	10.5	10.5	<i>n</i> -butylamine	13.1	13.7
4-methoxyaniline	16.5	15.8	<i>N</i> -methylglycinenitrile	13.5	13.9
4-methoxypyridine	11.4	12.2	<i>N</i> -methylmorpholine	16.4	16.8
4-nitroimidazole (anion)	11.4	11.5	<i>N</i> -methylpropargylamine	13.5	13.5
4-pyrrolidinopyridine	13.4	15.5	<i>n</i> -propylamine	13.3	13.6
4-pyridone (anion)	14.8	15.1	perhydroazepine	18.3	16.6
9-methylguanine (anion)	10.8	10.2	piperazine	17.2	17.8
adenine (anion)	10.4	10.5	piperidine	18.1	16.4
allylamine	13.2	12.5	propargylamine	12.3	11.7
ammonia	9.5	9.7	<i>p</i> -toluidine	13.0	12.9
aniline	13.0	12.2	purine (anion)	11.0	9.9
benzotriazole (anion)	11.5	11.7	pyridine	11.1	11.1
benzylamine	13.4	12.3	pyrrolidine	17.2	15.9
diethylamine	14.7	15.7	semicarbazide	11.0	10.2
dimethylamine	17.1	15.6	<i>tert</i> -butylamine	10.5	13.1
ethanolamine	12.6	13.3	theophylline (anion)	10.1	10.2
ethylamine	12.9	13.5	thymine (anion)	11.7	12.9

^aExperimental (exptl) and calculated (calcd) values are reported. ^bFrom ref 46.

action fields (MIFs) of the protein and those created by the substrate.⁴⁴ Since the flexibility of both the substrate and FMO3 is of fundamental importance, the method used has been designed in such a way to reproduce poses that are similar to experimentally determined poses in a precise and rapid manner. In fact, FLAP is capable of evaluating tens of thousands of poses in a fraction of a second. Figure 8A shows the flow diagram of the algorithm. The shape of the protein cavity is precisely evaluated through the use of the GRID force field^{45,27} in a dynamic manner, which is considering the enzyme as a flexible object in such a way that the shape of the cavity can be modified or chosen by the substrate itself. This is similar in concept to having more than one cavity being made available by the single FMO3 enzyme.

Simultaneously, each substrate is modeled in different conformations, all of which are used to generate all the possible energetically favorable poses of the substrate inside the cavity. An energetically favorable enzyme–substrate interaction is obtained when a molecule in a defined conformation possesses many atoms that can be superimposed onto the MIFs of the enzyme (refer to Figure 8B). The function evaluates the degree of superposition of all the poses. At the end of the process, the most probable pose (the one showing the best superposition) will be evident from the comparison of all the poses inside all the possible cavities. Even so, it is not only the single best pose in terms of enzyme–substrate fields similarity that is chosen, but a given number of optimal poses are memorized and analyzed. Indeed, it might often happen that the best exposition of the reactive center is not for a very reactive atom, which could lead to a slow reaction. Better kinetics could be obtained for a pose with a lower similarity score, which however exposes a more reactive atom in the active site.

The study of all the optimal poses (refer to the computational details) is also necessary in order to predict whether a compound can be considered to be a substrate of FMO3 or not. From the analysis of the data obtained from a collection of 95 FMO3 substrates and 50 nonsubstrates, two important facts have emerged. First, in order for a xenobiotic compound to be considered a substrate of FMO3, it must possess at least one group with a nucleophilic value that is higher than a defined threshold, as reported in the next paragraph. Second, the substrate must also be able to form at least one geometrically efficient interaction with the enzyme. This interaction is evaluated through the similarity of the interaction fields and must be assigned a value that is equal to or higher than a defined threshold. Obviously if a large number of virtually reactive poses are found, that compound will have a higher probability of being a substrate of FMO3.

Calculation of the Nucleophilicity of the Substrate. A nucleophile is an atom, ion, or molecule that has an electron pair that may be donated in forming a covalent bond to an electrophile (or Lewis acid). Polar and protic solvents, such as water, solvate anions by hydrogen bonding interactions. The solvated species are more stable and less reactive than the unsolvated “naked” anions. Therefore, nucleophilicity in water depends on the charge, polarizability, solvation, and HOMO energy of a chemical moiety. A set of 50 chemical compounds for which the experimentally measured nucleophilicity value (in water) is available⁴⁶ was used to correlate the experimental nucleophilicity value with a number of *in silico* calculated parameters, such as the nucleophile-atom charge, solvation, polarizability, and HOMO energy. PLS⁴⁷ was used to produce a chemometric model linking the *in silico* parameters to the experimental nucleophilicity values. The experimental nucleophile-reactivity parameters in water solvent are listed in Table 2,

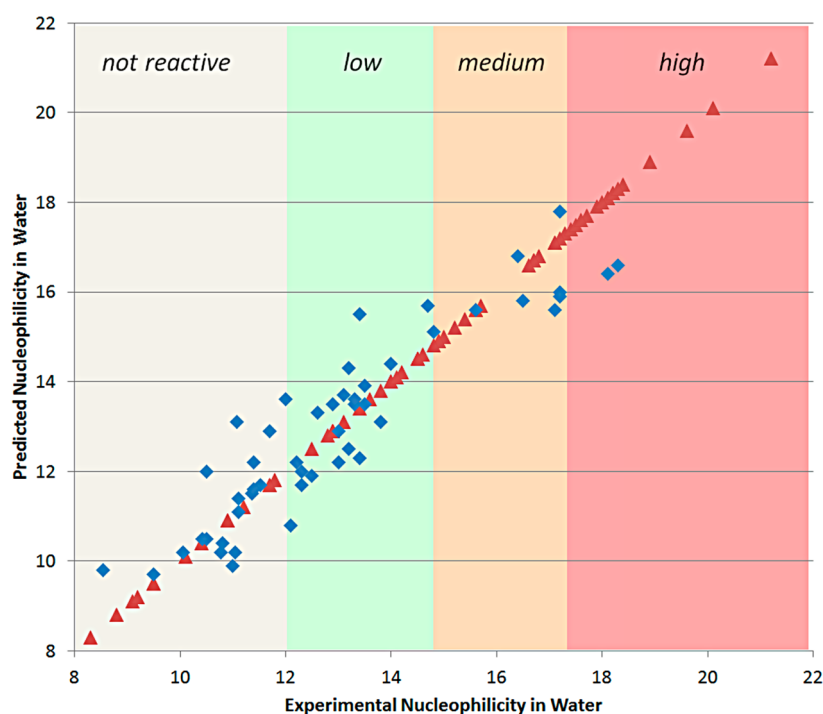


Figure 9. Experimental vs recalculated nucleophilicity (in water) for 50 chemical entities from Table 2 (in blue rhombus). The remaining 65 compounds (red triangles) lack experimental value and are predicted from nucleophilicity model (see methods section). The nucleophilicity range is arbitrarily divided into four regions (thresholds), from not reactive (when it is very low) to low, medium, and high nucleophilicity values.

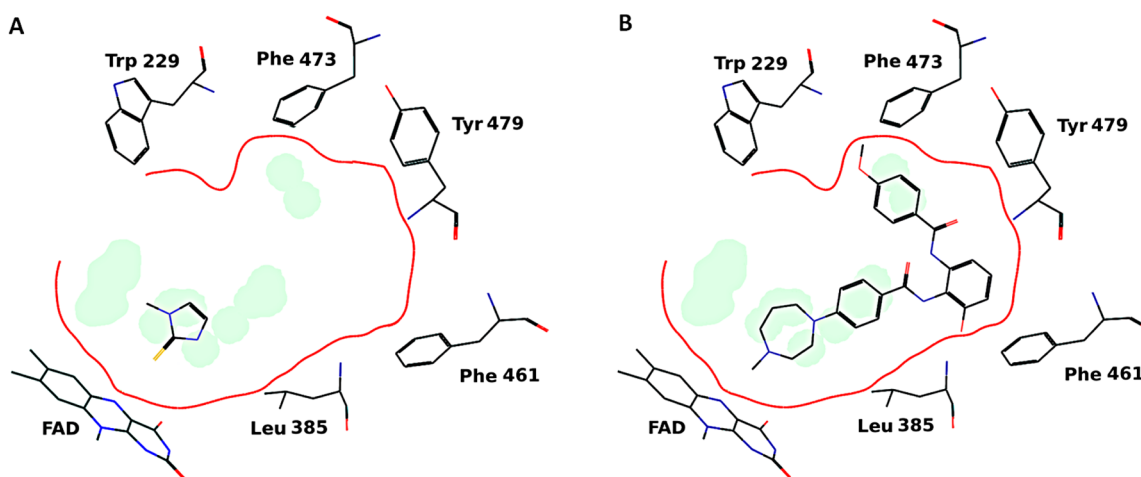


Figure 10. Reactivity equalization. (A) Small substrates can interact with FAD in different orientations, exposure constraints being practically absent. When two or more oxidation sites are possible, their nucleophilicity values will determine the oxidation rate and the metabolite's abundance. (B) Large substrates can be strongly constrained because of several interactions with the cavity. In this case exposure, rather than nucleophilicity, plays a relevant role in determining the site of metabolism.

together with the recalculated parameters obtained from the PLS model. The same model was later used to calculate the nucleophilicity in water of many different nucleophilic groups that are frequently used in medicinal chemistry for which the experimental values are not yet available. In this way it was possible to construct a nucleophile-reactivity scale for more than 115 small synthesizable compounds, all of which are potential substrates of FMO. When other factors are constant, this scale can be used to estimate the likelihood that a chemical group suffers an electrophilic attack by FMO enzymes. Figure 9 shows the model that relates the experimental and the recalculated nucleophile-reactivity values for all the data points

used in the training set and for the most diverse data points predicted in the test set.

Calculation of the SoM for FMO3. As with the cytochromes,⁴⁸ even in this case the oxidation reaction happens by a combination of substrate reactivity (described in this case by its nucleophilicity) and by the productive spatial interaction with the enzyme (favorable enzyme recognition).

Once the enzyme-accessibility and nucleophilic-reactivity components are calculated, the site of metabolism is described by a probability function P_{SoM} (probability for the site of metabolism), which is correlated to and can be considered to be an approximation of the free energy of the overall process.^{48,28} The two factors that contribute to the creation

of the P_{SoM} function in the original equation (recognition and reactivity) were equally weighed, though in reality their respective contributions very much depend on both the cytochrome/FMO being used and the substrate molecule.

Figure 10 illustrates an example of how this may happen when using different substrates with the same FMO enzyme. In “case A”, a substrate with a low molecular weight (methimazole) interacts with the FMO3 catalytic site. The substrate is smaller than the enzyme cavity and can interact with the reactive oxygen atom in many different ways. In this case, recognition is less important than the reactivity of the various fragments, and so the most reactive fragment is the most likely to be metabolized. “Case B” (with compound darexaban from Table 1) is an opposite example.

Here, the volume of the substrate is almost as large as that of the cavity itself. This is not so frequent for FMO but is common for P450 enzymes. Recognition is very important here because of the many different interactions that the substrate might have with the cavity. The reactivity of the fragments in this case is of minor importance when computing the SoM and only serves as a “corrective” role.

This example demonstrates that calculating the SoM using fixed weights for recognition and reactivity is conceptually wrong. It would be more correct to use weight coefficients (w_e and w_r in eq 1) that are based on the type of the enzyme cavity and the structure of the substrate. This feature in MetaSite5 is called reactivity equalization.²⁸ The use of this function allows the automatic recalculation of the weights in eq 1 to consider the enzyme cavity (which is determined by the type of CYP/FMO being used) and the interactions of the substrate with the amino acids within this cavity. One result of the reactivity-equalization function is that the weight coefficient of the reactivity component of the equation will be increased for small to medium substrates in large enzymes (CYP3A4) and decreased for medium to large molecules in enzymes with small cavities (i.e., CYP2E1, FMO3).

$$P_{\text{SoM},i} = (1 + w_e)E_i(1 + w_r)R_i \quad (1)$$

MetaSite Predictions. Once the reactivity and recognition models were introduced into MetaSite, this procedure was used to predict the isoform selectivity and the site of metabolism for a number of known and unknown xenobiotics, the experimental data of which have been produced in house. It was noticed that the prediction of isoform selectivity for voriconazole (17), sulfamethoxazole (18), dapson (19), and imipramine (20) (Figure 11) did not coincide with literature data.

The first three of these compounds are given as FMO3 substrates,^{49,50} while the last compound is an uncertain case because it has been reported to be both a substrate and a

nonsubstrate.^{14,15} Nevertheless, experiments performed using recombinant human FMO3 proved without a doubt that the predictions are correct, with the first three compounds being nonsubstrates of FMO3 and with imipramine being a good substrate. Regarding the compounds listed in Figure 6, MetaSite correctly predicts them as FMO3 substrates. However, while the first one is a good substrate (Figure 12), compounds 15 and 16 are metabolized in less amount with the experimental conditions used (Figure S2, Supporting Information). The site of metabolism prediction for the three substrates in Figure 6 is optimal. For these compounds, not only does MetaSite correctly predict the oxidized groups but it also correctly predicts their ranking (see Figure 12 and Supporting Information).

An even more interesting situation was the prediction of bepridil, of which no information concerning FMO3 metabolism was available. This drug was predicted to be a nonsubstrate, and the subsequent incubation with FMO3 verified the correct nature of the prediction. Nevertheless, it is still possible to use MetaSite to obtain information on which groups need to be modified/eliminated/added to enhance or reduce the interaction of a substrate with FMO3. In practice, by forcing the exposition of the potentially reactive group to the C4 α -hydroperoxide center, it is possible to obtain information on which part of the molecule needs to be modified to favor or disfavor a specific interaction. In the case of bepridil, the model proposed that if the oxidation of the pyridoline nitrogen were required, the lateral isobutoxy chain would need to be eliminated to favor the correct interaction, since this chain interacts repulsively with the Phe461 amino acid residue of FMO3 cavity and does not allow the correct orientation of the molecule for the oxidation reaction to occur. (Figure 13A).

The bepridil derivative called BPEA (benzyl[2-(1-pyrrolidinyl)ethyl]aniline) “suggested” by the computational procedure was synthesized and tested. In agreement with the MetaSite prediction, this derivative was found to be a good substrate of FMO3, and it also reacted in the predicted position, that is, oxidation of the pyridoline nitrogen (Figure 13B). Kinetic behavior for compound BPEA is reported in Figure 14.

CHEMISTRY

BPEA (benzyl[2-(1-pyrrolidinyl)ethyl]aniline, c) was synthesized according to Scheme 1. Nucleophilic replacement of bromide from 2-bromoethanol by pyrrolidine in refluxing acetonitrile, in the presence of potassium carbonate, afforded the amino alcohol a which was converted into the corresponding triflate b by reaction with triflic anhydride in dichloromethane. Finally, the target product c was obtained by reacting the alkyl triflate b with the sodium amide of *N*-benzylaniline in refluxing toluene.

CONCLUSIONS

Human FMO enzymes are a small family of highly active microsomal monooxygenases that primarily detoxify, and to a lesser extent bioactivate, xenobiotics containing nucleophilic centers. The literature search discussed in this paper revealed that the role of FMO enzymes has been underestimated, especially in the case of FMO3, which is the most dominant isoform in the liver. The LC/MS studies performed on a selected number of compounds proved useful for an improved understanding of the nature of FMO3 substrates and of the

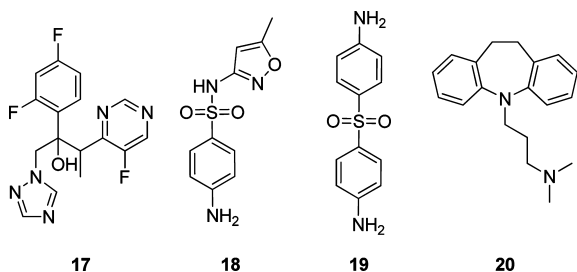


Figure 11. Structures of voriconazole (17), sulfamethoxazole (18), dapson (19), and imipramine (20).

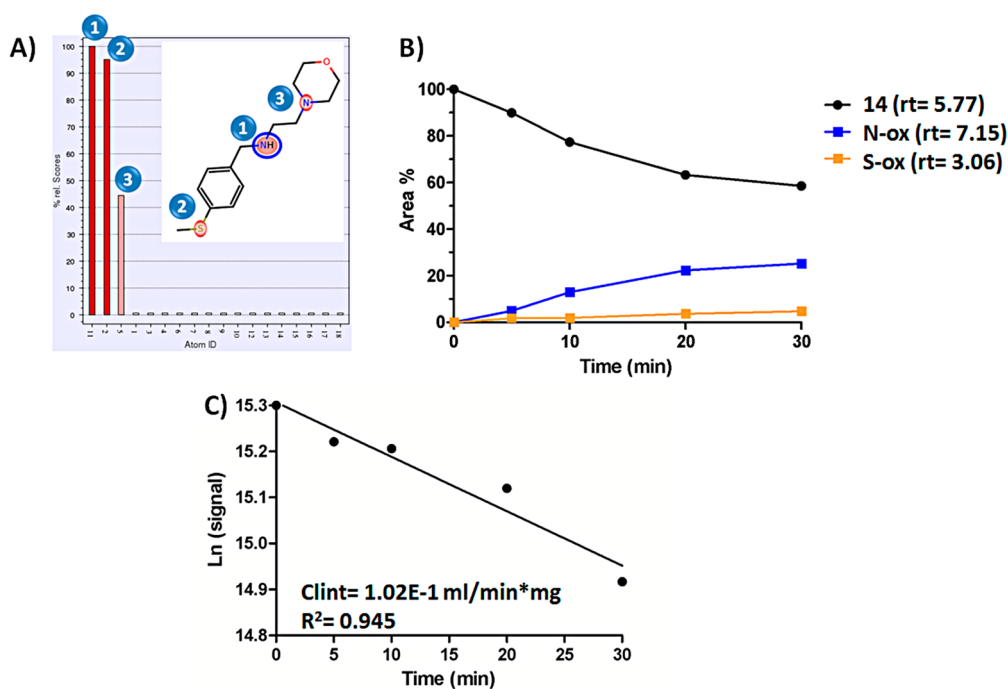


Figure 12. Comparison between predicted and experimental SoM for compounds 14. (A) MetaSite SoM prediction for compound 14. The highest oxidation probability (marked with 1) corresponds to the fastest N-oxidation reaction. S-oxidation is predicted to be the second most probable reaction (marked with 2). (B) In vitro metabolism study for compound 14. The N-oxidized metabolite at the benzylamine position and the S-oxidized metabolites are formed. (C) Clearance determination for compound 14.

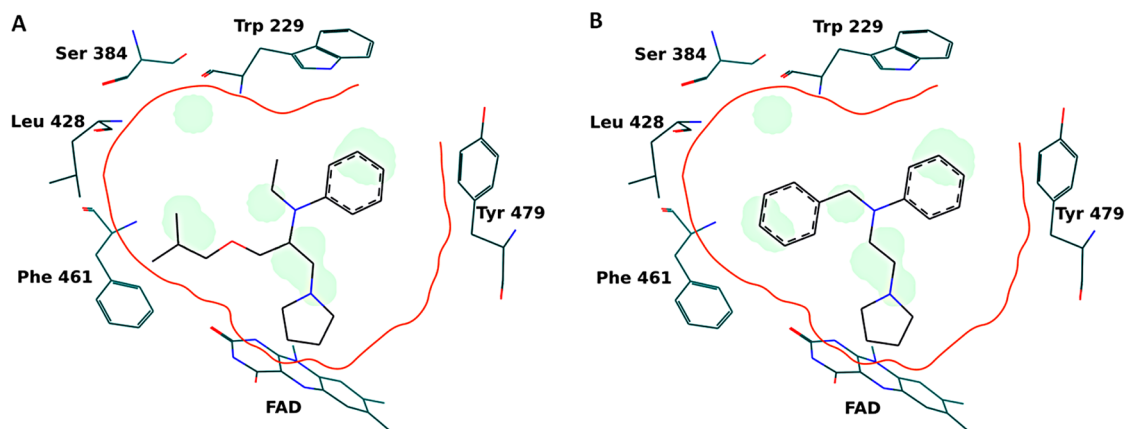


Figure 13. Our experimental data show that bepridil is not an FMO3 substrate. MetaSite reports that this may be due to steric clash (A) between the isopropoxy chain with the enzyme cavity. When the chain was synthetically removed, the new compound in (B) was a good FMO3 substrate with SoM in the predicted pyrrolidil nitrogen.

enzyme selectivity. This study therefore suggests that medicinal chemists should consider FMO metabolism during pharmaceutical development as they currently do for the cytochrome P450 (CYP) enzymes. To help the medicinal chemists in this task, it follows that in silico tools are required to aid design that also allow the prediction of FMO metabolism. Therefore, the most important of these enzymes, FMO3, was modeled starting from a bacterial analogue, with the aim of obtaining predictions on substrate selectivity and site of metabolism for all potential xenobiotics that interact with human FMO3. The procedure, once developed and inserted into the MetaSite software, correctly predicted more than 90% of the substrates known today for FMO3 (86 out of 95) and about 85% of the known nonsubstrates (42 out of 50). A high fidelity was also observed when predicting the site of metabolism, when used in the

presence of more than one potentially reactive groups. The SoM prediction for FMO3 in MetaSite has a 92% success rate (using top1 ranking scheme). It is interesting to note that in most cases in which the MetaSite prediction did not coincide with literature data (voriconazole, sulfamethoxazole, dapsone, imipramine) experiments demonstrated the correctness of the prediction. Moreover, MetaSite was able to guide the design of one FMO3 substrate, thus demonstrating that the procedure can be used to transform an FMO3 substrate into a nonsubstrate or vice versa and to eliminate or improve the clearance of potential substrates. We believe that computer aided drug metabolism elucidation (CADME), when applied to the isoform FMO3, can sensibly improve and hasten our understanding of the role of this enzyme in the clearance and eventual toxicity of the drug/xenobiotic compounds.

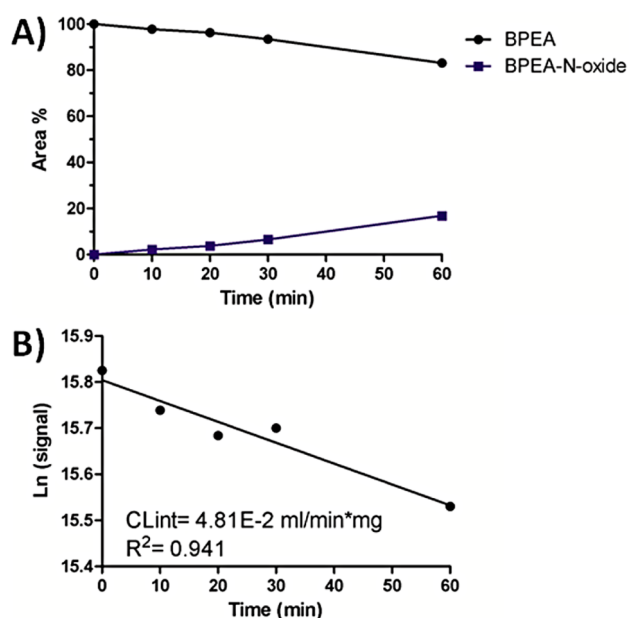


Figure 14. (A) BPEA depletion and BPEA N-oxide formation in human FMO3 enzyme. (B) Clearance data for BPEA.

EXPERIMENTAL SECTION

Materials. Diphenhydramine hydrochloride (2), cyamemazine (3), bepridil hydrochloride (4), tetrahydroisoquinoline (8), cimetidine (11), voriconazole (17), sulfamethoxazole (18), dapsone (19), and imipramine hydrochloride (20) were purchased from Sigma-Aldrich (St. Louis, MO). Compounds 9, 10, 12–17 were acquired from SPECS (www.specs.net). Human FMO3 supersomes (catalog number 456233), expressed in the baculovirus system, were purchased from BD Gentest (Woburn, MA).

Purities of the Acquired Compounds. Purity of the acquired compounds was determined by UHPLC on Agilent Technologies 6540 UHD Accurate Mass Q-TOF LC/MS, 1290 Infinity Series with DAD detector and evaluated to be higher than 95%. Chromatographic conditions to assess the purity of acquired or final compounds were as follows: column, Phenomenex Aeris peptide 2.1 mm \times 100 mm (1.7 μ m); flow rate, 0.3 mL/min; acquisition time, 20 min; DAD 190–650 nm; oven temperature, 45 $^{\circ}$ C; linear gradient of acetonitrile in water both containing 0.1% of formic acid (0–100% in 20 min).

Chemistry. Materials and Instrumentation. ^1H and ^{13}C NMR nuclear magnetic resonance (NMR) spectra were recorded at 400 and 100.6 MHz, respectively, on Bruker Avance II 400 MHz spectrometer at room temperature. Samples have been dissolved in deuteriochloroform. Chemical shifts (δ) are given in parts per million (ppm) relative to the internal standard tetramethylsilane. Peak multiplicities are reported as s (singlet), d (doublet), dd (double doublet), t (triplet), dt (double triplet), q (quartet), p (pentet), sept (septet), hept (heptet), m (multiplet), or br s (broad singlet). Coupling constants (J) are given in Hz. HRMS spectra were registered on Agilent Technologies 6540 UHD Accurate Mass Q-TOF LC/MS system. Purity of the final compound was determined by UHPLC and was $\geq 98\%$ pure.

2-Bromoethanol and pyrrolidine were commercial products (Aldrich) of the highest purity; they were used without further purification. Aniline (Aldrich) was freshly distilled at reduced pressure before use. *N*-Benzylaniline was prepared from benzaldehyde and aniline according to literature method.⁵¹ Acetonitrile and toluene were distilled from P_2O_5 . Air and moisture sensitive compounds were stored in Schlenk tubes or Schlenk burets. They were handled under an atmosphere of 99.995% pure nitrogen, using appropriate glassware.

Synthetic Procedures. Synthesis of benzyl[2-(1-pyrrolidinyl)ethyl]aniline (BPEA) was performed according to Scheme 1.

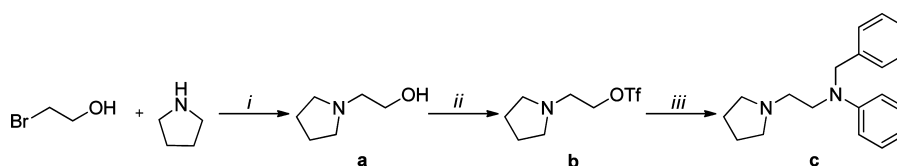
2-(Pyrrolidin-1-yl)ethanol (a).⁵² 2-Bromoethanol (3.5 mL, 50 mmol) in dry acetonitrile (25 mL) was added dropwise, under nitrogen atmosphere, to a refluxing mixture of pyrrolidine (4.4 mL, 53 mmol) and anhydrous powdered potassium carbonate (6.2 g, 45 mmol) in dry acetonitrile (75 mL). After 15 h, the mixture was allowed to cool to 25 $^{\circ}$ C, the solid was filtered off, washed with AcOEt, and the solvent was evaporated at reduced pressure. Flash chromatography on silica gel (eluent, 8:2 dichloromethane/methanol mixture) allowed collection of the expected product as a yellow oil (3.6 g, 31 mmol, 62% yield) exhibiting the following characteristics: ^1H NMR (CDCl_3) δ 4.22 (br s, 1H), 3.66 (t, $J = 1.6$ Hz, 2H), 2.70 (t, $J = 1.6$ Hz, 2H), 2.64 (br s, 4H), 1.80 (br s, 4H); ^{13}C NMR (CDCl_3) δ 59.6, 57.8, 54.0 (2C), 23.4 (2C); HRMS calcd for $\text{C}_6\text{H}_{13}\text{NO}$ 116,1075 ($M + \text{H}^+$), found 116.1069 ($M + \text{H}^+$).

2-(Pyrrolidin-1-yl)ethyl Trifluoromethanesulfonate (b). Trifluoromethanesulfonic anhydride (0.16 mL, 0.96 mmol) was added to a solution of a (100 mg, 0.87 mmol) in dry DCM (1 mL) at -20 $^{\circ}$ C, under nitrogen atmosphere. After the cooling bath was removed, the mixture was stirred for 30 min at 25 $^{\circ}$ C. After solvent evaporation at reduced pressure, the residual brown oil was pure enough to be used in the following step without further purification.

***N*-Benzyl-*N*-(2-(pyrrolidin-1-yl)ethyl)aniline (BPEA, c).** *N*-Benzylaniline (0.3 mL, 1.74 mmol) was added to a stirred suspension of NaH (83 mg, 3.48 mmol) in dry toluene (1 mL) under nitrogen atmosphere. After hydrogen generation ceased, a solution of aminotriflate b (0.87 mmol) in dry toluene (1 mL) was added and the reaction mixture was refluxed overnight. Upon cooling at room temperature, the reaction was quenched with MeOH and H_2O , extracted with AcOEt, and the organic layer was dried over anhydrous Na_2SO_4 . After the solvent was evaporated at reduced pressure, chromatography of the residue on silica gel (eluent 95:5 DCM/MeOH mixture) allowed recovery of an orange oil (50 mg, 21% yield) exhibiting the following spectroscopic characteristics: ^1H NMR (CDCl_3) δ 7.24–7.21 (m, 2H), 7.18–7.09 (m, 5H), 6.67–6.60 (m, 3H), 4.49 (s, 2H), 3.56 (t, $J = 8.0$ Hz, 2H), 2.74 (t, $J = 8.0$ Hz, 2H), 2.60 (br s, 4H), 1.76 (br s, 4H); ^{13}C NMR (CDCl_3) δ 148.2, 138.7, 129.3 (2C), 128.6 (2C), 126.9, 126.6 (2C), 116.6, 112.4 (2C), 54.9, 54.5 (2C), 52.9, 49.7, 23.4 (2C); HRMS calcd for $\text{C}_{19}\text{H}_{24}\text{N}_2$ 281,2018 ($M + \text{H}^+$), found 281.2017 ($M + \text{H}^+$).

Drug Metabolism with Recombinant Human Flavin-Containing Monooxygenase FMO3. Substrates were preincubated for 5 min at 37 $^{\circ}$ C in a 50 mM glycine buffer (pH 9.5) with NADPH (1 mM) in a total volume of 250 μL . The reactions were initiated by addition of human FMO3 supersomes (100 μg) in a shaking water bath at 37 $^{\circ}$ C. Preliminary studies were performed incubating each compound at 0 and 30 min. A volume of 250 μL of cold acetonitrile (containing 0.6 μM labetalol as an internal standard) was added to the

Scheme 1^a



^aReagents and conditions: (i) K_2CO_3 , CH_3CN , 82 $^{\circ}$ C; (ii) Tf_2O , DCM, rt; (iii) *N*-benzylaniline, NaH, 60% dispersion in mineral oil, toluene, 110 $^{\circ}$ C.

mix to terminate the reaction. Proteins were precipitated by centrifugation at 12 000g for 5 min at 4 °C, and aliquots of the supernatants were analyzed by LC–MS/MS as described in the next paragraph. Compounds proved to be substrates for FMO3 were further investigated, repeating the assay with more incubation times (0, 5, 10, 20, and 30 min). Structural elucidation of the metabolites by MSMS data and Cl_{int} evaluation were automatically performed by Mass-MetaSite software (Molecular Discovery).^{53,54} Theoretical and experimental molecular ion mass, elemental composition, mass error, characteristic fragments, and retention times t_R for substrates and metabolites are reported as Supporting Information. To determine the potential metabolic products formed by the FMO3 enzyme for voriconazole, sulfamethoxazole, and dapsone, which were previously reported to be FMO3 substrates, FMO3 in different concentrations (100, 500 μ g) was incubated with the individual substrates (5, 50, 100 μ M concentrations) in the presence of NADPH (2 mM) for 5, 10, 20, 30, and 60 min. No metabolites were formed in all of the analyses. The same conditions were used for all the other nonsubstrates tested in this paper.

Analytical Equipment and Methods. The LC/MS analyses were run on a Agilent 6540 UHD accurate mass Q-TOF LC/MSMS system governed by Agilent MassHunter software (B.05.00 version). The system consists of a binary pump, autosampler, thermostated column compartment, DAD detector, source, and Q-TOF spectrometer. A volume of 2 μ L of each sample was injected by the autosampler. Chromatographic separation of the metabolites was performed on the two chromatographic conditions indicated in Table 3. In both cases

Table 3. LC Methods Used for Metabolism Studies

column	gradient	flow rate (mL/min)
Method a		
Aeris widepore 3.6 μ m C4, 100 mm \times 4.6 mm (Phenomenex, USA)	time 0 min, B 0%	0.45
	time 15 min, B 15%	
	time 18 min, B 100%	
	time 20 min, stop run	
Method b		
Aeris peptide 1.7 μ m XB-C18, 100 mm \times 2.1 mm (Phenomenex, USA)	time 0 min, B 0%	0.3
	time 20 min, B 100%	
	time 20 min, stop run	

the mobile phases consisted of A ($H_2O/0.1\%$ formic acid) and B (acetonitrile/ 0.1% formic acid) and the columns were operating at a constant temperature of 40 °C. Compounds **3**, **8–10**, **12–16** were acquired with method a, and all the other compounds were acquired with method b.

The DAD detector stored all the acquired spectra in the 190–640 nm range (2 nm spectrum step). The ion source was an Agilent Dual JetStream operating under positive ionization mode (4000 V), with nitrogen as desolvating gas (320 °C, 10 L/min, 35 psig). The fragmentor was set to 110 V, the skimmer to 65 V, and the octapole rf to 750 V. The spectrometric data were collected in AutoMSMS mode in the 100–1000 mass range, with 3 scans/s both in MS and in MS/MS scans. The TOF operated at 2 GHz.

Computational Section. The starting structure of human FMO3 was built with the homology modeling web server I-TASSER^{55,56} which used as templates different bacterial FMO3 structures (PDB codes 2vq7, 3gwd, 3ucl, 2xve).

The model was then subjected to minimization, equilibration, and a 50 ns long MD simulation. The standard protonation state at physiological pH was assigned to ionizable residue. Parameters for the FADH2 and NADP+ cofactors were obtained with antechamber using the bcc charging methodology. Waters and ions were added with tleap.⁵⁷ In particular, the structure was immersed in a pre-equilibrated

cubic box of TIP3P⁵⁸ water molecules, and the final system contained around 23 100 waters.

MD simulations were run using Gromacs 4.6.1.⁵⁹ The LINCS algorithm⁶⁰ was used for constraining all bonds. Trajectories were collected in the NVT ensemble using periodic boundary conditions and Ewald sums for long-range electrostatic interactions. The system was first minimized with the steepest descent algorithm and then equilibrated by heating from 100 to 300 K in three 100 ps steps at 100, 200, and 300 K. Finally, a 50 ns production trajectory was run, collecting frames at 2 ps intervals. Each of the MD snapshots extracted using normal-mode analysis was submitted to FLAP analysis to find the surface binding pockets and the corresponding protein-snapshot pharmacophoric features. The procedure was repeated for all of the protein snapshots and the single pharmacophoric features were collected in a unique global “dynamic pharmacophore” model. Finally, the global pharmacophore was used as a template in a structure based approach inside the MetaSite algorithm.⁴⁸

MIF and Similarity Calculation. The GRID force field²⁷ was used to produce molecular interaction fields (MIFs) inside the FMO active site. The program GRID is calibrated in a water environment to obtain chemically specific information about a macromolecule (in this case the human FMO3). An electrostatic potential does not normally allow favorable binding sites to be differentiated for a primary, secondary, or tertiary amine cation, for pyridinium, or for a carboxy anion, so the GRID method is an attempt to compute analogous potentials that do have chemical specificity. The object used to measure the potential at each point is given the generic name “Probe”. Many different Probes can be used on the same macromolecule one after another, and each represents a specific chemical group. A great deal of chemically specific information can therefore be accumulated concerning the way in which the macromolecule might interact favorably with other ligand molecules.

The MIFs in the binding sites of the human FMO3 were obtained using the flexible mode in GRID. With the flexible option, the amino acid side chains can automatically move in response to attractive or repulsive interactions with the chemical probe. The side chain flexibility in GRID can mimic the amino acid movements that occur in the CYP active site to accommodate different substrates according to their sizes, shapes, and interaction patterns.

Nucleophilicity Calculation. A set of more than 50 molecules for which the experimentally measured nucleophilicity value (in water) is available was used to create a model correlating these experimentally derived values to the charge, solvation, polarizability, and HOMO energy of the same molecules. The structures have been preliminary relaxed at a semiempirical level using the Austin model 1 (AM1) theory. The resulting geometries have been further optimized with density functional theory (DFT) method at the B3LYP/6-31+G* level of theory in the presence of water. The solvation effect of water has been treated by self-consistent reaction field (SCRf) and the CPCM polarizable conductor calculation model. HOMO, MEP potential, frequencies, and exact polarizability have been computed at the same level of theory using the software Spartan.⁶¹ Once computed, the charge, solvation, polarizability, and HOMO energy were correlated with the experimental nucleophilicity using the PLS chemometric tool. The maximum prediction power, estimated by the LOO technique, was obtained using one latent variable. This variable explained 90% of the Y variance. The same procedure was then repeated from the beginning for new chemical groups for which the nucleophilicity values in water are not available. The test set molecules were projected into the previously developed PLS model in order to obtain the predictions of the nucleophilicity values.

■ ASSOCIATED CONTENT

📄 Supporting Information

Metabolism of diphenhydramine in FMO3, CYP2D6 and CYP3A4; metabolism of compounds **15** and **16** in FMO3; main metabolites identified in FMO3 by HRMS; molecular formula strings (in SMILES) for all the molecules investigated

in csv format. This material is available free of charge via the Internet at <http://pubs.acs.org>.

AUTHOR INFORMATION

Corresponding Author

*G.C.: phone, +39 075 585 5629; fax, +39 075 45646; e-mail, gabriele.cruciani@unipg.it.

Notes

The authors declare no competing financial interest.

ACKNOWLEDGMENTS

The authors thank Prof. Andrea Mattevi (Pavia University, Italy) for the assistance provided during the work on the crystalline structure 2vq7 and the Fondazione Cassa Risparmio Perugia (Project Code No. 2012.0138.021) and “FIRB-Futuro in Ricerca 2010” Program (Project RBFR10X500) for their financial support.

ABBREVIATIONS USED

CADME, computer aided drug metabolism elucidation; FMO, flavin containing monooxygenase; SoM, site of metabolism; CYP450, cytochrome P450; MIF, molecular interaction field; FLAP, fingerprint for ligands and proteins; MetaSite, site of metabolism calculation; MetID, metabolite identification; MAO, monoaminooxidase; NADPH, nicotinamide adenine dinucleotide phosphate; FAD, flavin adenine dinucleotide; PLD, phospholipidosis; PDB, Protein Data Bank; PLS, partial least squares; AM1, Austin model 1; DFT, density functional theory; SCRF, self-consistent reaction field; LOO, leave one out; DCM, dichloromethane; BPEA, benzyl[2-(1-pyrrolidinyl)-ethyl]aniline

REFERENCES

- (1) Cashman, J. R. Human flavin-containing monooxygenase: substrate specificity and role in drug metabolism. *Curr. Drug Metab.* **2000**, *1*, 181–191.
- (2) Cashman, J. R.; Zhang, J. Human flavin-containing monooxygenases. *Annu. Rev. Pharmacol. Toxicol.* **2006**, *46*, 65–100.
- (3) Ziegler, D. M.; Pettit, F. H. Microsomal oxidases. I. The isolation and dialkylarylamine oxygenase activity of pork liver microsomes. *Biochemistry* **1966**, *5*, 2932–2938.
- (4) Testa, B.; Pedretti, A.; Vistoli, G. Reactions and enzymes in the metabolism of drugs and other xenobiotics. *Drug Discovery Today* **2012**, *17*, 549–560.
- (5) Deng, P.; Zhong, D.; Yu, K.; Zhang, Y.; Wang, T.; Chen, X. Pharmacokinetics, metabolism, and excretion of the antiviral drug arbidol in humans. *Antimicrob. Agents Chemother.* **2013**, *57*, 1743–1755.
- (6) Capolongo, F.; Santi, A.; Anfossi, P.; Montesissa, C. Benzydramine as a useful substrate of hepatic flavin-containing monooxygenase activity in veterinary species. *J. Vet. Pharmacol. Ther.* **2009**, *33*, 341–346.
- (7) Hanlon, S. P.; Camattari, A.; Abad, S.; Glieder, A.; Kittelmann, M.; Lütz, S.; Wirz, B.; Winkler, M. Expression of recombinant human flavin monooxygenase and moclobemide-N-oxide synthesis on multi-mg scale. *Chem. Commun.* **2012**, *48*, 6001–6003.
- (8) Mushiroda, T.; Douya, R.; Takahara, E.; Nagata, O. The involvement of flavin-containing monooxygenase but not CYP3A4 in metabolism of itopride hydrochloride, a gastroprokinetic agent: comparison with cisapride and mosapride citrate. *Drug Metab. Dispos.* **2000**, *28*, 1231–1237.
- (9) Chung, W. G.; Park, C. S.; Roh, H. K.; Lee, W. K.; Cha, Y. N. Oxidation of ranitidine by isozymes of flavin-containing monooxygenase and cytochrome P450. *Jpn. J. Pharmacol.* **2000**, *84*, 213–220.
- (10) Söderberg, M. M.; Dahl, M. L. Pharmacogenetics of olanzapine metabolism. *Pharmacogenomics* **2013**, *14*, 1319–1336.
- (11) Lohr, J. W.; Willsky, G. R.; Acara, M. A. Renal drug metabolism. *Pharmacol. Rev.* **1998**, *50*, 107–141.
- (12) Ring, B. J.; Wrighton, S. A.; Aldridge, S. L.; Hansen, K.; Haehner, B.; Shipley, L. A. Flavin-containing monooxygenase-mediated N-oxidation of the M(1)-muscarinic agonist xanomeline. *Drug Metab. Dispos.* **1999**, *27*, 1099–1103.
- (13) Cashman, J. R.; Celestial, J. R.; Leach, A.; Newdell, J.; Park, S. B. Tertiary amines related to brompheniramine: preferred conformations for N-oxygenation by the hog liver flavin-containing monooxygenase. *Pharm. Res.* **1993**, *10*, 1097–1105.
- (14) Hernandez, D.; Janmohamed, A.; Chandan, P.; Omar, B. A.; Phillips, I. R.; Shephard, E. A. Deletion of the mouse Fmo1 gene results in enhanced pharmacological behavioural responses to imipramine. *Pharmacogenet. Genomics* **2009**, *19*, 289–299.
- (15) Adali, O.; Carver, G. C.; Philpot, R. M. Modulation of human flavin-containing monooxygenase 3 activity by tricyclic antidepressants and other agents: importance of residue 428. *Arch. Biochem. Biophys.* **1998**, *358*, 92–97.
- (16) Akutsu, T.; Kobayashi, K.; Sakurada, K.; Ikegaya, H.; Furihata, T.; Chiba, K. Identification of human cytochrome p450 isozymes involved in diphenhydramine N-demethylation. *Drug Metab. Dispos.* **2007**, *35*, 72–78.
- (17) Ziegler, D. M. Flavin-containing monooxygenases: catalytic mechanism and substrate specificities. *Drug Metab. Rev.* **1988**, *19*, 1–32.
- (18) Krueger, S. K.; Williams, D. E. Mammalian flavin-containing monooxygenases: structure/function, genetic polymorphisms and role in drug metabolism. *Pharmacol. Ther.* **2005**, *106*, 357–387.
- (19) Goracci, L.; Ceccarelli, M.; Bonelli, D.; Cruciani, G. Modeling phospholipidosis induction: reliability and warnings. *J. Chem. Inf. Model.* **2013**, *53*, 1436–1446.
- (20) Orogo, A. M.; Choi, S. S.; Minnier, B. L.; Kruhlak, N. L. Construction and consensus performance of (Q)SAR models for predicting phospholipidosis using a dataset of 743 compounds. *Mol. Inf.* **2012**, *31*, 725–739.
- (21) Zhou, L.; Geraci, G.; Hess, S.; Yang, L.; Wang, J.; Argikar, U. Predicting phospholipidosis: a fluorescence non cell based in vitro assay for the determination of drug phospholipid complex formation in early drug discovery. *Anal. Chem.* **2011**, *83*, 6980–6987.
- (22) Quagliano, D.; Ha, H. R.; Duner, E.; Bruttomesso, D.; Bigler, L.; Follath, F.; Realdi, G.; Pettenazzo, A.; Baritussio, A. Effects of metabolites and analogs of amiodarone on alveolar macrophages: structure–activity relationship. *Am. J. Physiol.: Lung Cell. Mol. Physiol.* **2004**, *287*, 438–447.
- (23) Shiraga, T.; Kaneko, H.; Iwasaki, K.; Tozuka, Z.; Suzuki, A.; Hata, T. Identification of cytochrome P450 enzymes involved in the metabolism of zotepine, an antipsychotic drug, in human liver microsomes. *Xenobiotica* **1999**, *29*, 217–229.
- (24) Giri, S.; Krausz, K. W.; Idle, J. R.; Gonzalez, F. J. The metabolomics of (+/–)-arecoline 1-oxide in the mouse and its formation by human flavin-containing monooxygenases. *Biochem. Pharmacol.* **2007**, *73*, 561–573.
- (25) Jensen, K. G.; Dalgaard, L. In vitro metabolism of the m1-muscarinic agonist 5-(2-ethyl-2H-tetrazol-5-yl)-1-methyl-1,2,3,6-tetrahydropyridine by human hepatic cytochromes p-450 determined at pH 7.4 and 8.5. *Drug Metab. Dispos.* **1999**, *27*, 125–132.
- (26) Lin, J.; Cashman, J. R. N-oxygenation of phenethylamine to the trans-oxime by adult human liver flavin-containing monooxygenase and retroreduction of phenethylamine hydroxylamine by human liver microsomes. *J. Pharmacol. Exp. Ther.* **1997**, *282*, 1269–1279.
- (27) Carosati, E.; Sciabola, S.; Cruciani, G. Hydrogen bonding interactions of covalently bonded fluorine atoms: from crystallographic data to a new angular function in the GRID force field. *J. Med. Chem.* **2004**, *47*, 5114–5125.
- (28) Cruciani, G.; Baroni, M.; Benedetti, P.; Goracci, L.; Fortuna, C. G. Exposition and reactivity optimization to predict sites of

- metabolism in chemicals. *Drug Discovery Today: Technol.* **2013**, *10*, e155–e165.
- (29) Shiraga, T.; Yajima, K.; Teragaki, T.; Suzuki, K.; Hashimoto, T.; Iwatsubo, T.; Miyashita, A.; Usui, T. Identification of enzymes responsible for the N-oxidation of darexaban glucuronide, the pharmacologically active metabolite of darexaban, and the glucuronidation of darexaban N-oxides in human liver microsomes. *Biol. Pharm. Bull.* **2012**, *35*, 413–421.
- (30) Jacobsen, W.; Christians, U.; Benet, L. Z. In vitro evaluation of the disposition of A novel cysteine protease inhibitor. *Drug Metab. Dispos.* **2000**, *28*, 1343–1351.
- (31) Ohmi, N.; Yoshida, H.; Endo, H.; Hasegawa, M.; Akimoto, M.; Higuchi, S. S-oxidation of S-methyl-esonarimod by flavin-containing monooxygenases in human liver microsomes. *Xenobiotica* **2003**, *33*, 1221–1231.
- (32) Xie, G.; Wong, C. C.; Cheng, K. W.; Huang, L.; Constantinides, P. P.; Rigas, B. Regioselective oxidation of phospho-NSAIDs by human cytochrome P450 and flavin monooxygenase isoforms: implications for their pharmacokinetic properties and safety. *Br. J. Pharmacol.* **2012**, *16*, 222–232.
- (33) Attar, M.; Dong, D.; Ling, K. H.; Tang-Liu, D. D. Cytochrome P450 2C8 and flavin-containing monooxygenases are involved in the metabolism of tazarotenic acid in humans. *Drug Metab. Dispos.* **2003**, *31*, 476–481.
- (34) Kajita, J.; Inano, K.; Fuse, E.; Kuwabara, T.; Kobayashi, H. Effects of olopatadine, a new antiallergic agent, on human liver microsomal cytochrome P450 activities. *Drug Metab. Dispos.* **2002**, *30*, 1504–1511.
- (35) Ripp, S. L.; Overby, L. H.; Philpot, R. M.; Elfarra, A. A. Oxidation of cysteine S-conjugates by rabbit liver microsomes and cDNA-expressed flavin-containing mono-oxygenases: studies with S-(1,2-dichlorovinyl)-L-cysteine, S-(1,2,2-trichlorovinyl)-L-cysteine, S-allyl-L-cysteine, and S-benzyl-L-cysteine. *Mol. Pharmacol.* **1997**, *51*, 507–515.
- (36) Dever, J. T.; Elfarra, A. A. In vivo metabolism of L-methionine in mice: evidence for stereoselective formation of methionine-d-sulfoxide and quantitation of other major metabolites. *Drug Metab. Dispos.* **2006**, *34*, 2036–2043.
- (37) el Amri, H. S.; Fargetton, X.; Delatour, P.; Batt, A. M. Sulphoxidation of albendazole by the FAD-containing and cytochrome P-450 dependent mono-oxygenases from pig liver microsomes. *Xenobiotica* **1987**, *17*, 1159–1168.
- (38) Furnes, B.; Schlenk, D. Extrahepatic metabolism of carbamate and organophosphate thioether compounds by the flavin-containing monooxygenase and cytochrome P450 systems. *Drug Metab. Dispos.* **2005**, *33*, 214–218.
- (39) Milletti, F.; Storchi, L.; Sforza, G.; Cruciani, G. New and original pK_a prediction method using grid molecular interaction fields. *J. Chem. Inf. Model.* **2007**, *47*, 2172–2181.
- (40) Cruciani, G.; Milletti, F.; Storchi, L.; Sforza, G.; Goracci, L. In silico pK_a prediction and ADME profiling. *Chem. Biodiversity* **2009**, *6*, 1812–1821.
- (41) Alfieri, A.; Malito, E.; Orru, R.; Fraaije, M. W.; Mattevi, A. Revealing the moonlighting role of NADP in the structure of a flavin-containing monooxygenase. *Proc. Natl. Acad. Sci. U.S.A.* **2008**, *105*, 6572–6577.
- (42) Koukouritaki, S. B.; Poch, M. T.; Henderson, M. C.; Siddens, L. K.; Krueger, S. K.; VanDyke, J. E.; Williams, D. E.; Pajewski, N. M.; Wang, T.; Hines, R. N. Identification and functional analysis of common human flavin-containing monooxygenase 3 genetic variants. *J. Pharmacol. Exp. Ther.* **2007**, *320*, 266–273.
- (43) Baroni, M.; Cruciani, G.; Sciabola, S.; Perruccio, F.; Mason, J. S. A common reference framework for analyzing/comparing proteins and ligands. Fingerprints for ligands and proteins (FLAP): theory and application. *J. Chem. Inf. Model.* **2007**, *47*, 279–294.
- (44) Sirci, F.; Goracci, L.; Rodríguez, D.; van Muijlwijk-Koezen, J.; Gutiérrez-de-Terán, H.; Mannhold, R. Ligand-, structure- and pharmacophore-based molecular fingerprints: a case study on adenosine A(1), A (2A), A (2B), and A (3) receptor antagonists. *J. Comput.-Aided Mol. Des.* **2012**, *26*, 1247–1266.
- (45) Goodford, P. J. The basic principles of GRID. In *Molecular Interaction Fields: Applications in Drug Discovery and ADME Prediction*; Cruciani, G., Ed.; Wiley-VCH: Weinheim, Germany, 2006; pp 1–25.
- (46) Mayr's Database of Reactivity Parameters. <http://www.cup.lmu.de/oc/mayr/reaktionsdatenbank/fe/showclass/40> (accessed February 1, 2014).
- (47) Rosipal, R.; Kramer, N. Overview and recent advances in partial least squares. In *Subspace, Latent Structure and Feature Selection: Statistical and Optimization Perspectives Workshop (SLSFS 2005)*; Saunders, C., et al., Eds.; Springer-Verlag: New York, 2006; pp 34–51.
- (48) Cruciani, G.; Carosati, E.; De Boeck, B.; Ethirajulu, K.; Mackie, C.; Howe, T.; Vianello, R. MetaSite: understanding metabolism in human cytochromes from the perspective of the chemist. *J. Med. Chem.* **2005**, *48*, 6970–6979.
- (49) Yanni, S. B.; Annaert, P. P.; Augustijns, P.; Ibrahim, J. G.; Benjamin, D. K., Jr.; Thakker, D. R. In vitro hepatic metabolism explains higher clearance of voriconazole in children versus adults: role of CYP2C19 and flavin-containing monooxygenase 3. *Drug Metab. Dispos.* **2010**, *38*, 25–31.
- (50) Vyas, P. M.; Roychowdhury, S.; Koukouritaki, S. B.; Hines, R. N.; Krueger, S. K.; Williams, D. E.; Nauseef, W. M.; Svensson, C. K. Enzyme-mediated protein haptentation of dapsone and sulfamethoxazole in human keratinocytes: II. Expression and role of flavin-containing monooxygenases and peroxidases. *J. Pharmacol. Exp. Ther.* **2006**, *319*, 497–505.
- (51) Alinezhad, H.; Tajbakhsh, M.; Mahdavi, N. One-pot reductive amination of carbonyl compounds using sodium borohydride-amberlist 15. *Synth. Commun.* **2010**, *40*, 951–956.
- (52) O'Connor, S.; Dumas, J.; Lee, W.; Dixon, J.; Cantin, D.; Gunn, D.; Burke, J.; Phillips, B.; Lowe, D.; Shelekhin, T.; Wang, G.; Ma, X.; Ying, S.; McClure, A.; Achebe, F.; Lobell, M.; Ehgott, F.; Iwuagwu, C.; Parcella, K. Pirrolo[2,1-F][1,2,4]triazin-4-ylamines IGF-1R kinase inhibitors for the treatment of cancer and other hyperproliferative diseases. U.S. Patent US20110294776 A1, Dec 1, 2011.
- (53) Bonn, B.; Leandersson, C.; Fontaine, F.; Zamora, I. Enhanced metabolite identification with MS(E) and a semi-automated software for structural elucidation. *Rapid Commun. Mass Spectrom.* **2010**, *24*, 3127–3138.
- (54) Zamora, I.; Fontaine, F.; Serra, B.; Plasencia, G. High-throughput, fully automated, specific MetID. A revolution for drug discovery. *Drug Discovery Today: Technol.* **2013**, *10*, e199–205.
- (55) Zhang, Y. I-TASSER server for protein 3D structure prediction. *BMC Bioinf.* **2008**, *9*, 40.
- (56) I-TASSER Online. <http://zhanglab.ccmb.med.umich.edu/I-TASSER/> (accessed February 12, 2014).
- (57) Case, D. A.; Darden, T. A.; Cheatham, T. E., III; Simmerling, C. L.; Wang, J.; Duke, R. E.; Luo, R.; Walker, R. C.; Zhang, W.; Merz, K. M.; Roberts, B.; Hayik, S.; Roitberg, A.; Seabra, G.; Swails, J.; Goetz, A. W.; Kolossvary, I.; Wong, K. F.; Paesani, F.; Vanicek, J.; Wolf, R. M.; Liu, J.; Wu, X.; Brozell, S. R.; Steinbrecher, T.; Gohlke, H.; Cai, Q.; Ye, X.; Wang, J.; Hsieh, M.-J.; Cui, G.; Roe, D. R.; Mathews, D. H.; Seetin, M. G.; Salomon-Ferrer, R.; Sagui, C.; Babin, V.; Luchko, T.; Gusarov, S.; Kovalenko, A.; Kollman, P. A. *AMBER 12*; University of California: San Francisco, CA. 2012.
- (58) Jorgensen, W. L.; Chandrasekhar, J.; Madura, J. D.; Impey, R. W.; Klein, M. L. Comparison of simple potential functions for simulating liquid water. *J. Chem. Phys.* **1983**, *79*, 926–935.
- (59) Hess, B.; Kutzner, C.; van der Spoel, D.; Lindahl, E. GROMACS 4: algorithms for highly efficient, load-balanced, and scalable molecular simulation. *J. Chem. Theory Comput.* **2008**, *4*, 435–447.
- (60) Hess, B.; Bekker, H.; Berendsen, H. J. C.; Fraaije, J. G. E. M. Lincs: a linear constraint solver for molecular simulations. *J. Comput. Chem.* **1997**, *18*, 1463–1472.
- (61) Shao, Y.; Molnar, L. F.; Jung, Y.; Kussmann, J.; Ochsenfeld, C.; Brown, S. T.; Gilbert, A. T. B.; Slipchenko, L. V.; Levchenko, S. V.; O'Neill, D. P.; DiStasio, R. A., Jr.; Lochan, R. C.; Wang, T.; Beran, G. J. O.; Besley, N. A.; Herbert, J. M.; Lin, C. Y.; Van Voorhis, T.; Chien, S.

H.; Sodt, A.; Steele, R. P.; Rassolov, V. A.; Maslen, P. E.; Korambath, P. P.; Adamson, R. D.; Austin, B.; Baker, J.; Byrd, E. F. C.; Dachselt, H.; Doerksen, R. J.; Dreuw, A.; Dunietz, B. D.; Dutoi, A. D.; Furlani, T. R.; Gwaltney, S. R.; Heyden, A.; Hirata, S.; Hsu, C.-P.; Kedziora, G.; Khalliulin, R. Z.; Klunzinger, P.; Lee, A. M.; Lee, M. S.; Liang, W. Z.; Lotan, I.; Nair, N.; Peters, B.; Proynov, E. I.; Pieniazek, P. A.; Rhee, Y. M.; Ritchie, J.; Rosta, E.; Sherrill, C. D.; Simmonett, A. C.; Subotnik, J. E.; Woodcock, H. L., III; Zhang, W.; Bell, A. T.; Chakraborty, A. K.; Chipman, D. M.; Keil, F. J.; Warshel, A.; Hehre, W. J.; Schaefer, H. F.; Kong, J.; Krylov, A. I.; Gill, P. M. W.; Head-Gordon, M. Advances in methods and algorithms in a modern quantum chemistry program package. *Phys. Chem. Chem. Phys.* **2006**, *8*, 3172–3191.